Supplementary information

Tailoring the Optoelectronic Properties of MoO_X Nanoparticles: A Novel Microwave-Assisted Synthesis for Near-Infrared Absorbing Polyoxometallic Clusters

Daniel Truchan[a,b], Adriana Hvizdošová Annušová[a,c,d]*, Guilhem Curé[e], Matej Mičušík[d], Vojtech Nádaždy[a], Mário Kotlár[f], Giulia C. Fadda[b, g], Peter Nádaždy[a], Matej Jergel[a], Claire Wilhelm[e], Aurore Van de Walle[e], Peter Šiffalovič[a,c] and Yoann Lalatonne[b,h]*

[a] *Institute of Physics, Slovak Academy of Sciences, Dúbravská cesta 9, 845 11 Bratislava, Slovakia*

[b] *Laboratory for Vascular Translational Science, LVTS, INSERM, UMR 1148, Bobigny, France – Université Sorbonne Paris Nord (Paris 13), Université Paris Cité*

[c] *Centre for Advanced Materials Application, Slovak Academy of Sciences, Dúbravská cesta 9, 845 11 Bratislava, Slovakia*

[d] *Polymer Institute, Slovak Academy of Sciences, Dúbravská cesta 9, 845 41 Bratislava, Slovakia*

[e] *Laboratoire Physico Chimie Curie, CNRS UMR168, Institut Curie, Sorbonne Université, PSL University, 75005 Paris, France*

[f] *Centre for Nanodiagnostics of Materials, Slovak University of Technology in Bratislava, Vazovova 5, 812 43 Bratislava, Slovakia*

[g] *Laboratoire Léon Brillouin, CEA/CNRS UMR 12, CEA Saclay, 91191 Gif-sur-Yvette, France*

[h] *Biophysics and Nuclear Medicine department, Avicenne Hospital AP-HP, F-93009 Bobigny, France*

*E-mail: yoann.lalatonne@aphp.fr, adriana.hvizdosova.annusova@savba.sk

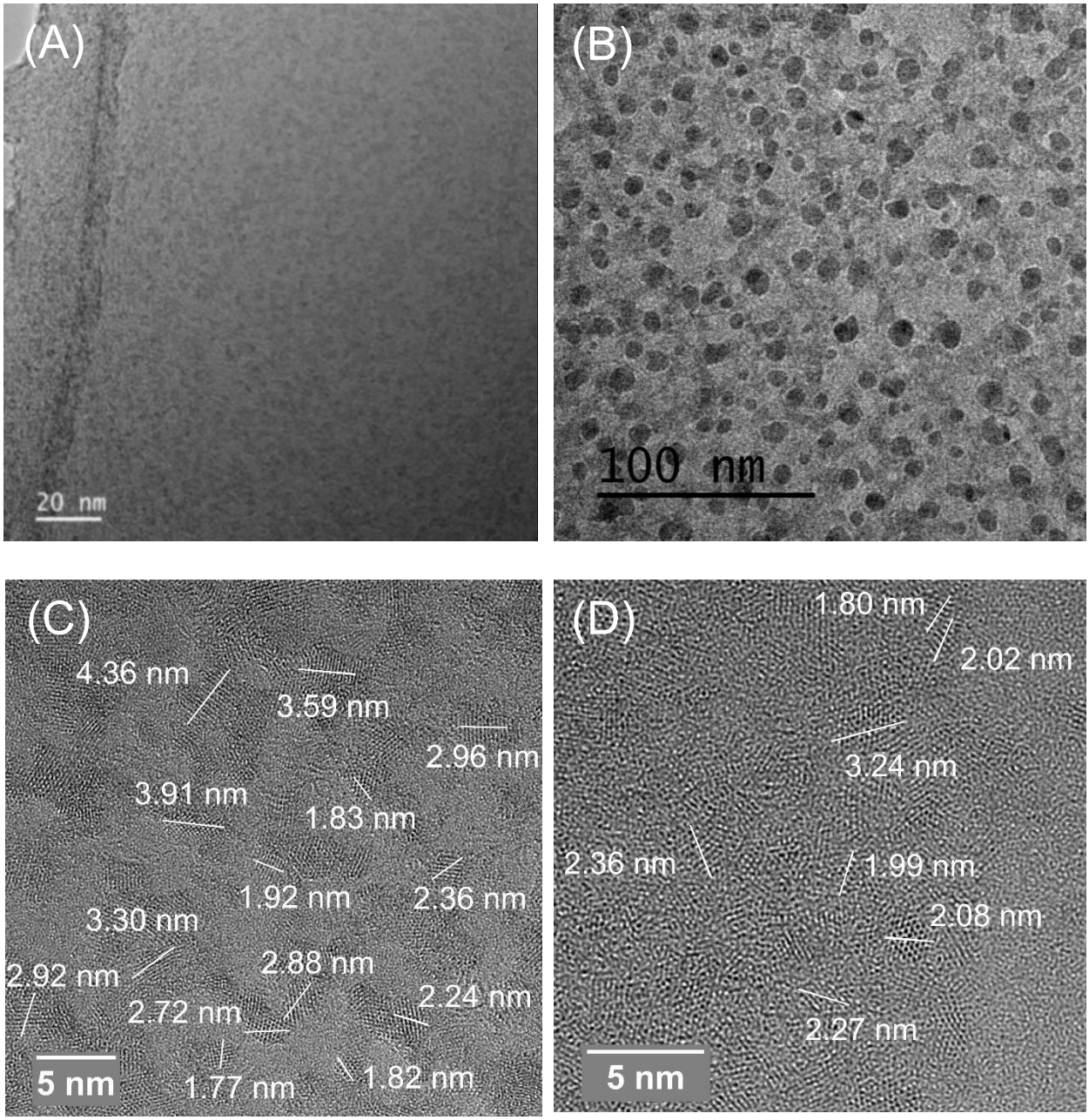

Figure S1 TEM micrographs for nanoparticles synthesized at higher temperatures under different conditions. Synthesis duration was 60 minutes at 150 °C (A) and 175 °C (B). Synthesis duration was 5 minutes at 120 °C (C) and 210 °C (D) – size is not affected by elevated temperature (for size-distribution histograms see Figure 2B in the Main text). Both long synthesis time and high temperature are needed for formation of bigger MoO_X nanoparticles during the microwave assisted synthesis. However, these do not exhibit photothermal properties.

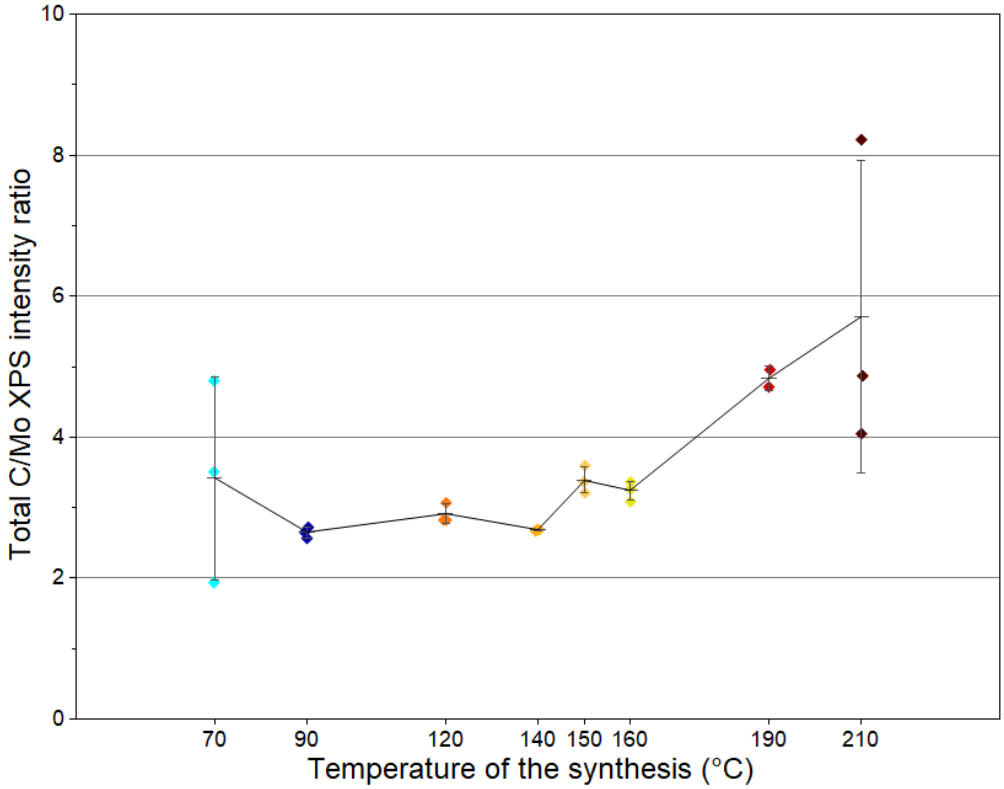

Figure S2 Total XPS-signal ratio of Carbon and Molybdenum (total sum of relative carbon- and molybdenum-associated signals). With the temperature increasing from 90 °C, organics constitute larger and larger part of the prepared product. Linear line connects means (± SD).

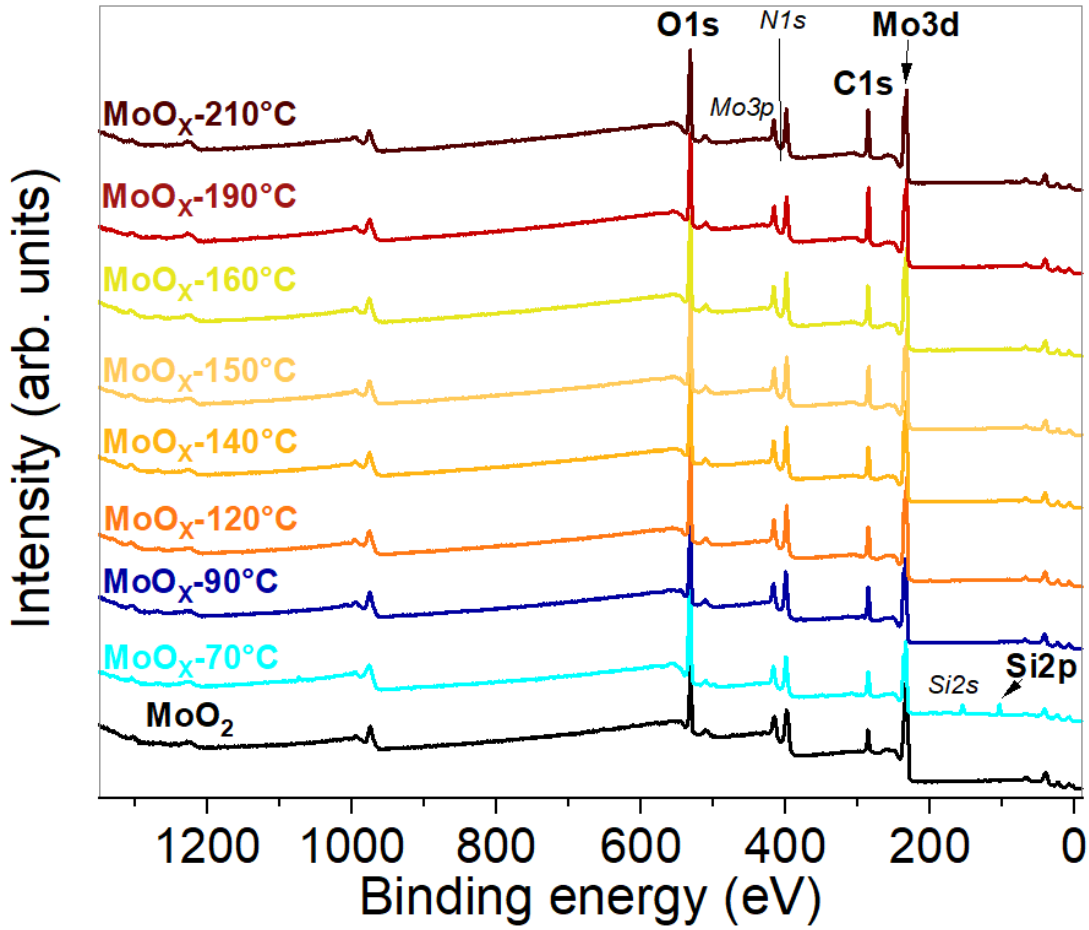

Figure S3 XPS survey of microwave-synthesized MoO_X samples prepared at different temperatures.

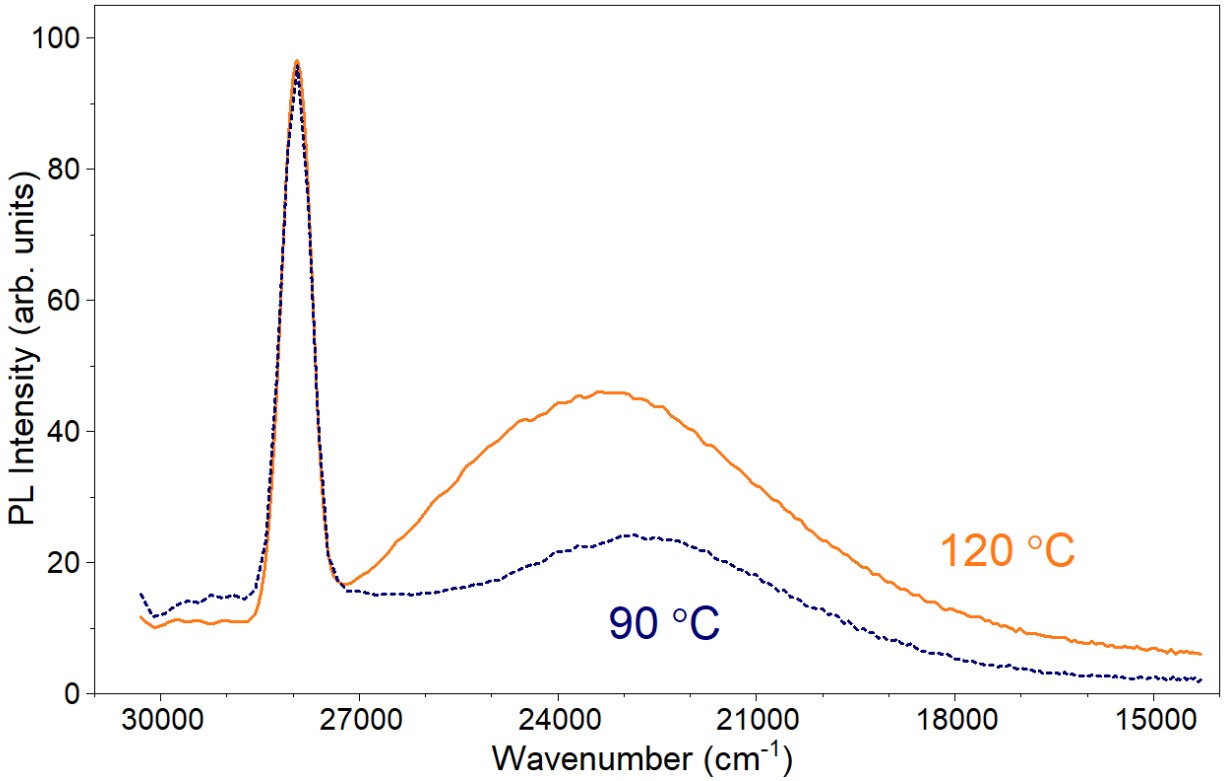

Figure S4 Photoluminescence emission spectra of samples prepared at 90 °C and 120 °C at the excitation wavelength of 320 nm (31 250 cm^{-1}). Only weak photoluminescence signal is present centered around 23 000 cm^{-1} (435 nm) – 120 °C sample exhibits more than 2 times greater photoluminescence compared to 90 °C. When excited, samples synthesized at lower temperatures are more prone to undergo non-radiative relaxation processes. Intensities were normalized in regard to Raman water peak at 28 950 cm^{-1} (358 nm).

Detailed FTIR analysis

Fourier-transform infrared (FTIR) spectroscopy provided crucial qualitative insight into the synthesis processes and mechanisms. Especially for nanoparticles, chemical structure can be deducted for prepared products, including crystallinity, types and multiplicity of chemical bonds and their particular arrangement. This information complements TEM information about size and morphology. Contrary to TEM, FTIR spectroscopy uncovered variations in the spectrum depending on the temperature of synthesis. Figure S5 shows the FTIR spectra for the microwave-synthesized MoO_X nanoparticles prepared at temperatures 70, 90, 120, 140, and 190 °C. Molybdenyl acetylacetonate (the precursor molecule) and MoO_3 microcrystalline powder are used as references. MoO_2 is not presented, as it does not provide IR peaks due to its symmetric bond structure. The most prominent effect of the preparation temperature is visible at the wavenumbers corresponding to the Mo=O stretching band around 1005 cm^{-1}. With increasing temperature, the peak position shifts from 1024 cm^{-1} for precursor molybdenyl acetylacetonate, through 1021 cm^{-1} and 1023 cm^{-1} for the synthesis temperature of 70 °C and 90 °C, 1024 cm^{-1} and 1020 cm^{-1} for 120 °C and 140 °C, up to 1004 cm^{-1} for 190 °C synthesis. In microcrystalline MoO_3, the peak remains at 988 cm^{-1} wavenumbers with increasing temperature (however, the maximum shift of ~25 cm^{-1} needed a temperature difference of 350 °C by this method,).[1]

The variable position of the Mo=O peak was well-documented in literature where Mo=O stretching vibrations were reported at 971 and 997 cm^{-1} in MoO_2Cl_2[2] but reached up to 1015 cm^{-1} in $MoOCl_4$[3] for gaseous phase. This dispersion of values was also reported by the density functional theory computations where positions of the Mo=O stretching vibration ranged from 980 to 1046 cm^{-1} [4] depending on the method. Interestingly, a similar value dispersion was observed for MoO_3 powder heated in a hydrogen atmosphere at different temperatures, where the peak position shifted to lower wavenumbers with increasing temperature[1].

Concerning the other spectral features, the peaks in the 960 – 700 cm^{-1} region correspond to Mo-O vibrations, which can be attributed to MoO_6 octahedral unit structure and its specific symmetry[5]. In this case, one Mo atom is adjacent to a couple of more distant O atoms at 2.24 and 2.31 Å and a quartet of closer O atoms with bond lengths ranging from 1.67 to 1.95 Å, resulting in two prominent peaks in the region[6]. The first group of oxygen atoms corresponds to the peak at 913 cm^{-1} while the other manifests as the peak at 895 cm^{-1} for the 190 °C product. For the samples synthesized at lower temperatures, the peaks are only very weak until the synthesis temperature of 140 °C is reached, when they become distinct. The peak positions are shifted by ~20 cm^{-1} to higher wavenumbers in the precursor spectrum, although the twin peak is clearly distinguishable. Another structural subunit described for Mo-O complexes is tetrahedral MoO_4 unit. In the case of perfect symmetry, it gives an estimated peak position at 858 cm^{-1} which matches a broad peak of the 190 °C synthesis product. This peak is totally absent for low and moderate temperatures, evidencing the absence of tetrahedral arrangement. We can deduce that whereas the octahedral arrangement is present in all products throughout the tested range of temperatures, the tetrahedral arrangement is specific for the high-temperature syntheses. In this spectral area, the precursor exhibits a prominent peak at around 800 cm^{-1} which indicates Mo-OH stretch[3] well-justified by the molecular structure. Contrary to the total absence of a peak at this position for the samples prepared at higher temperatures, weak peaks indicating Mo-OH stretches are present for the products of 70 °C and 90 °C syntheses. The peak prominence is greatly reduced after releasing the molybdenum-oxygen complexes from the organic part during synthesis.

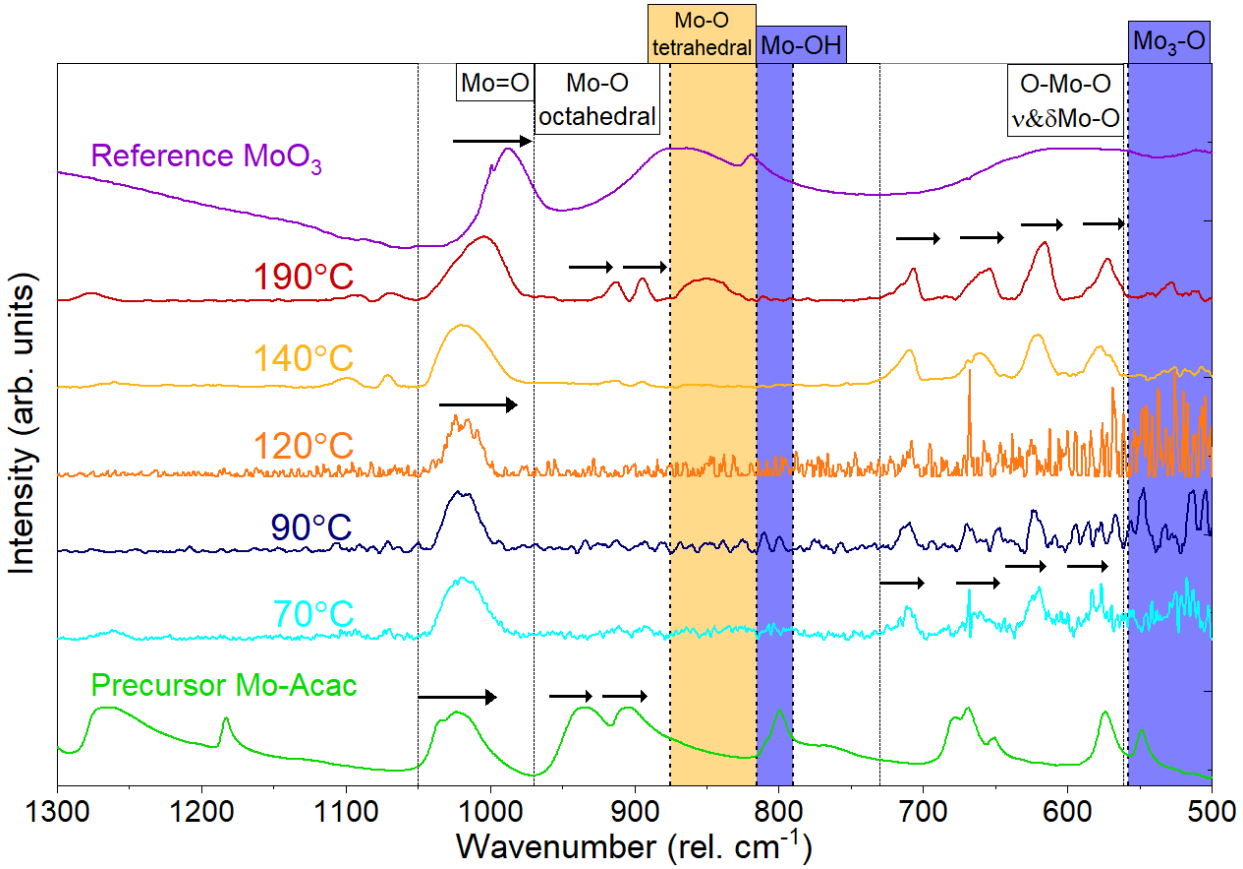

Figure S5 Low-wavenumber Fourier-transform infrared spectroscopy (FTIR) (in absorption) of the MoO_X nanoparticles synthesized by the microwave-assisted synthesis at different temperatures and comparison with the spectrum of precursor molecule MoO_2Acac and microcrystalline MoO_3 sample. The shifts to lower wavenumbers are apparent for several peaks (Mo=O, Mo-O octahedral ranges and a range hosting O-Mo-O along with ν- and δ- Mo-O vibrations). High-temperature-specific Mo-O tetrahedral vibration is denoted in orange, whereas low-temperature specific vibrations are highlighted by blue. Intensity curves are shifted in the y-direction for clarity.

The other peaks in the sub-1000 cm^{-1} region are present as well, mostly due to the plethora of Mo-O bond lengths and their vibrations, whose complete analysis is not in the scope of this study. An excellent overview of Mo-O IR information is presented in the work of Bart et al.[7]. Most importantly, a quartet of peaks at 579, 621, 663, and 712 cm^{-1} is present in practically all samples with a slight, gradual, temperature-dependent redshift reaching 5 cm^{-1} for the 190 °C sample (the shift of the 663 cm^{-1} peak reached even 10 cm^{-1}), similar to the position shifts in the Mo=O stretching band. For the products synthesized at the temperatures up to 120 °C, a richer band structure is observed between 600 and 540 cm^{-1} with a multitude of narrow peaks. Especially, the 90 °C sample exhibits an array of intense and narrow peaks with separate 668 and 648 cm^{-1} peaks replacing a single broad one centered at 663 cm^{-1}. Additionally, a single strong band is observed at 550 cm^{-1}. Some of the narrow peaks in this region suggest the bond energies restricted to a quite narrow bond not unlike in a crystal.

Concerning the wavenumbers over 1000 cm^{-1}, all prepared samples as well as references manifest a single weak band in the Mo=O overtone region[8] at 1965 cm^{-1} (Figure S6). Small contrast of the peak does not allow observation of its position shifting to lower wavenumbers analogous to the fundamental. Rich presence of different stretching O-H vibrations is visible at the wavenumbers over 3600 cm^{-1} (Figure S6)

owing to the presence of free (structural) O-H groups well-known throughout metal-oxide matrices[9]. Interestingly, its relative intensity is significantly decreased for the 190 °C sample in comparison to its other peaks, which is not the case for any other sample prepared at lower temperatures. Typical liquid water O-H stretching at 3400 cm^{-1} [10] is absent. In addition to this common feature, 190 °C product exhibits broad peak from 1640 to 1420 cm^{-1} (Figure 6) mixed from different C-C, C-O and C-OH vibrations, originating partly from residual acetylacetone[11] and partly from biphenyl linkage[12]. These can be observed when organic moiety is incorporated into nanoparticle structure during benzyl alcohol-mediated syntheses[13].

In general, we can conclude from FTIR that increasing temperature during microwave-assisted synthesis promotes the organization of Mo and O atoms from octahedral to more rigid tetrahedral structural subunits joined together into a sheet structure (Figure S5). Bands related to Mo-OH and Mo_3O vibrations were identified prominently in low-temperature synthesized samples. Additionally, Mo=O stretching position shifts with increasing temperature to lower sub-1000 cm^{-1} and temperature-dependent shifts in various Mo-O bond position are present as well. Apart from these, no other systemic and gradual changes were distinguished throughout the spectra at the set of temperatures.

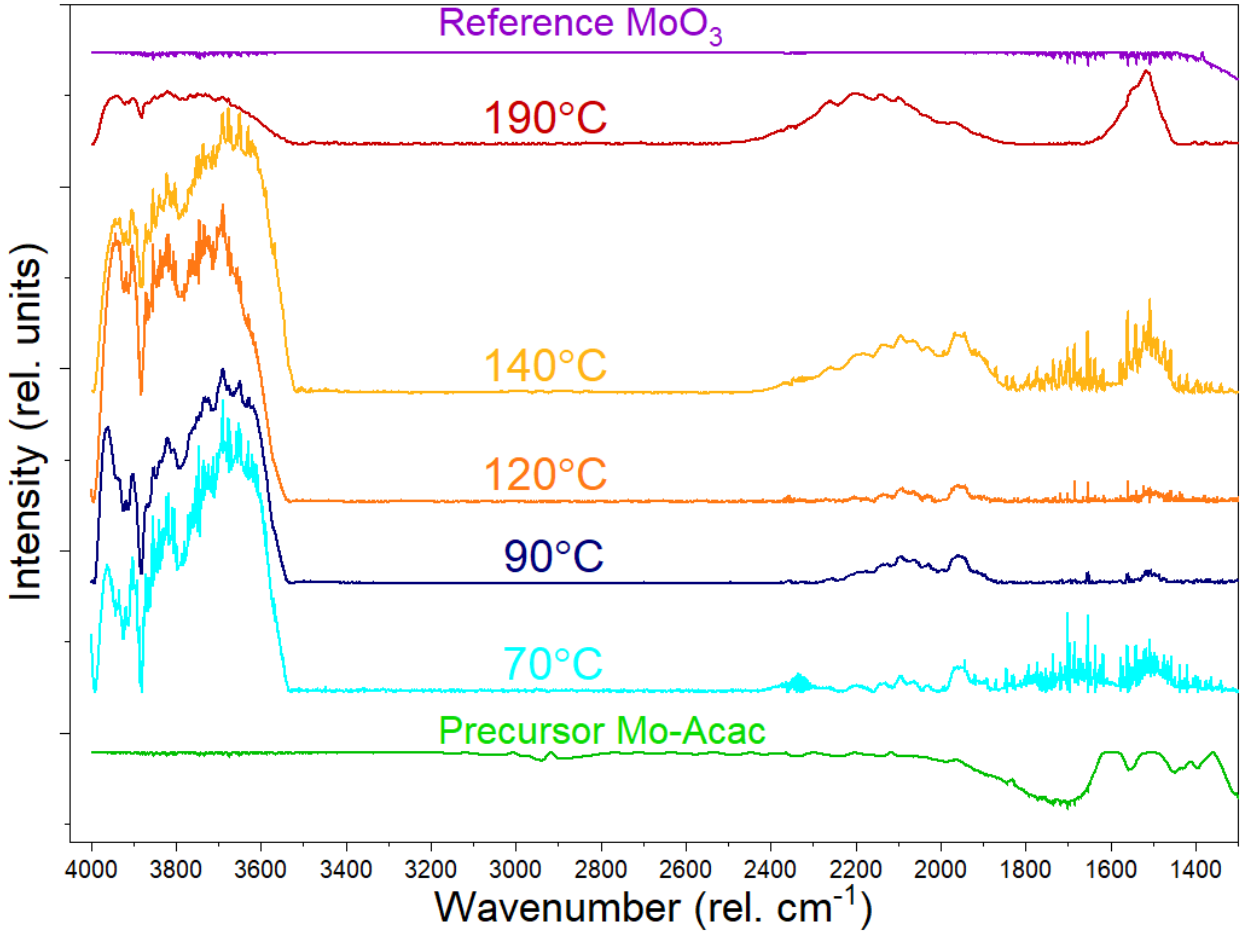

Figure S6 High-wavenumber FTIR region absorption spectra of the MoO_X sample prepared at different temperatures with MoO_3 and precursor molecule Molybdenyl acetylacetonate as references. Typical liquid water O-H stretching at 3400 cm^{-1} is absent in the samples although structural O-H vibrations are abundant at all samples with a notable exception for the MoO_X prepared at 190 °C. Mo=O vibration overtone is well-distinguishable at 1965 cm^{-1} in all samples as well as in the precursor. Intensity curves are shifted in the y-direction for clarity.

References for the FTIR analysis

(1) Hirata, T. In-Situ Observation of Mo-O Stretching Vibrations during the Reduction of MoO3 with Hydrogen by Diffuse Reflectance FTIR Spectroscopy. *Appl. Surf. Sci.* **1989**, *40* (1), 179–181. https://doi.org/10.1016/0169-4332(89)90174-8.

(2) Neikirk, D. L.; Fagerli, J. C.; Smith, M. L.; Mosman, D.; Devore, T. C. The Infrared Spectra of the moOCl, moO2Cl2, WOCl, WO2Cl2, MoO2, MoO3 and Mo3O9 Gaseous Molecules. *J. Mol. Struct.* **1991**, *244*, 165–181. https://doi.org/10.1016/0022-2860(91)80154-V.

(3) Iorns, T. V.; Stafford, F. E. Infrared Spectra of Some Gaseous Molybdenum Oxides and Oxyhalides. *J. Am. Chem. Soc.* **1966**, *88* (21), 4819–4822. https://doi.org/10.1021/ja00973a011.

(4) Handzlik, J.; Ogonowski, J. Structure of Isolated Molybdenum(VI) and Molybdenum(IV) Oxide Species on Silica: Periodic and Cluster DFT Studies. *J. Phys. Chem. C* **2012**, *116* (9), 5571–5584. https://doi.org/10.1021/jp207385h.

(5) Kurumada, M.; Kaito, C. Change in IR Spectra of Molybdenum Oxide Nanoparticles Due to Particles Size or Phase Change. *J. Phys. Soc. Jpn.* **2006**, *75* (7), 074712. https://doi.org/10.1143/JPSJ.75.074712.

(6) Kuroiwa, Y.; Sato, N.; Sawada, A.; Negishi, S.; Negishi, H.; Aoyagi, S. Electron Charge Density Study on the Bonding Nature in MoO3. *J. Phys. Soc. Jpn.* **2003**, *72* (11), 2811–2815. https://doi.org/10.1143/JPSJ.72.2811.

(7) Bart, J. C. J.; Cariati, F.; Sgamellotti, A. Mixed-Valence Effects in Tellurium-Molybdenum Oxides. *Inorganica Chim. Acta* **1979**, *36*, 105–112. https://doi.org/10.1016/S0020-1693(00)89378-0.

(8) Tsilomelekis, G.; Boghosian, S. In Situ Raman and FTIR Spectroscopy of Molybdenum(VI) Oxide Supported on Titania Combined with 18O/16O Exchange: Molecular Structure, Vibrational Properties, and Vibrational Isotope Effects. *J. Phys. Chem. C* **2011**, *115* (5), 2146–2154. https://doi.org/10.1021/jp1098987.

(9) Chukanov, N. V.; Vigasina, M. F. Some Examples of the Use of IR Spectroscopy in Mineralogical Studies. In *Vibrational (Infrared and Raman) Spectra of Minerals and Related Compounds*; Chukanov, N. V., Vigasina, M. F., Eds.; Springer International Publishing: Cham, 2020; pp 1–17. https://doi.org/10.1007/978-3-030-26803-9_1.

(10) Backhouse, J. R.; Lowe, H. M.; Sinn, E.; Suzuki, S.; Woodward, S. Bromination of Molybdenum Carbonyls Revisited: Oxo Complexes and Routes to New Materials Chemistry. *J. Chem. Soc. Dalton Trans.* **1995**, No. 9, 1489–1495. https://doi.org/10.1039/DT9950001489.

(11) Čeponkus, J.; Platakytė, R.; Šablinskas, V.; Quintanilla, A. G. FTIR Study of Acetylacetone, D2-Acetylacetone and Hexafluoroacetylacetone–Water Complexes in Argon and Nitrogen Matrices. *Chemija* **2018**, *29* (1). https://doi.org/10.6001/chemija.v29i1.3639.

(12) Talbi, D.; Chandler, G. S. Theoretical Infrared Spectra of Biphenyl, Terphenyls and Tetraphenyls for Astrophysical Purposes. *J. Mol. Spectrosc.* **2012**, *275*, 21–27. https://doi.org/10.1016/j.jms.2012.04.008.

(13) Pinna, N. The “Benzyl Alcohol Route”: An Elegant Approach towards Organic–Inorganic Hybrid Nanomaterials. *J. Mater. Chem.* **2007**, *17* (27), 2769–2774. https://doi.org/10.1039/B702854G.

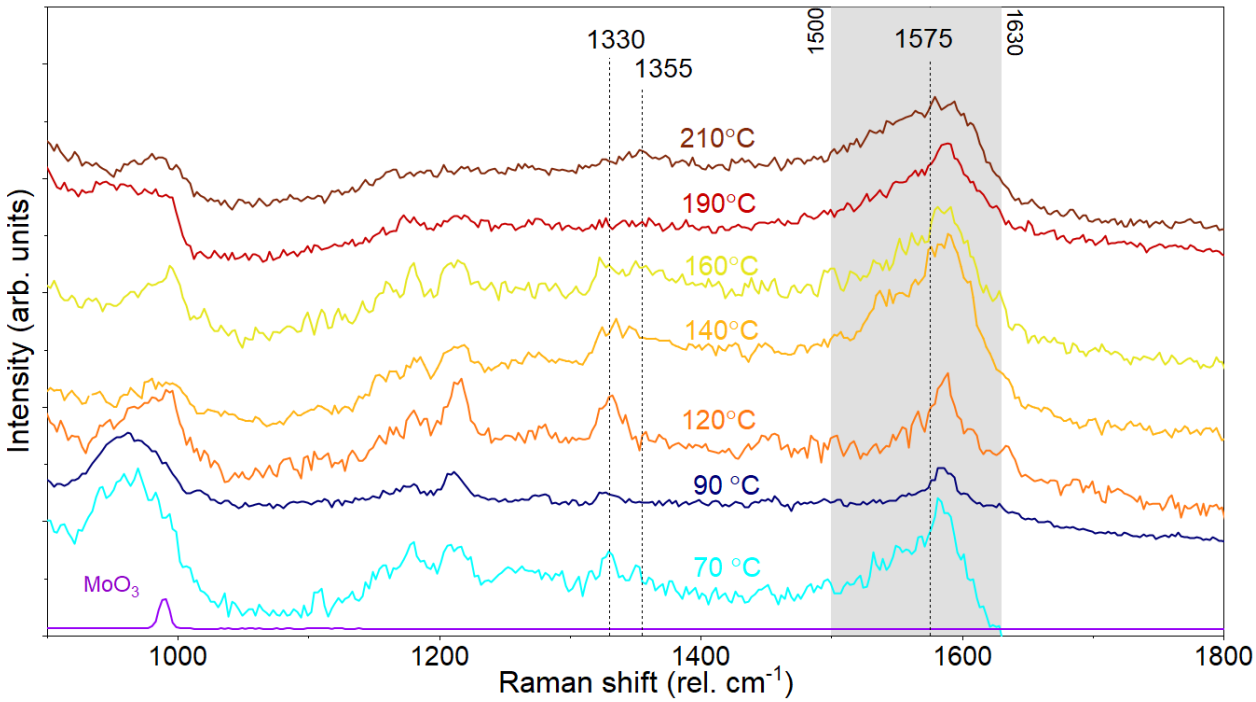

Figure S7 Raman spectra of microwave-assisted synthesis products prepared at Raman shifts associated with Carbon-related signals, Molybdenum does not provide Raman-active bonds in the area. Two carbon-associated peaks can be distinguished – D-band at around 1355 rel. cm^{-1} and G-band at 1575 rel. cm^{-1}. Drifting D-band position can be observed alternating from the 1355 and 1330 cm^{-1} position into sole peak at 1330 cm^{-1} and back to 1355 cm^{-1} for the highest temperatures. Intensity curves are shifted in y-direction for clarity.

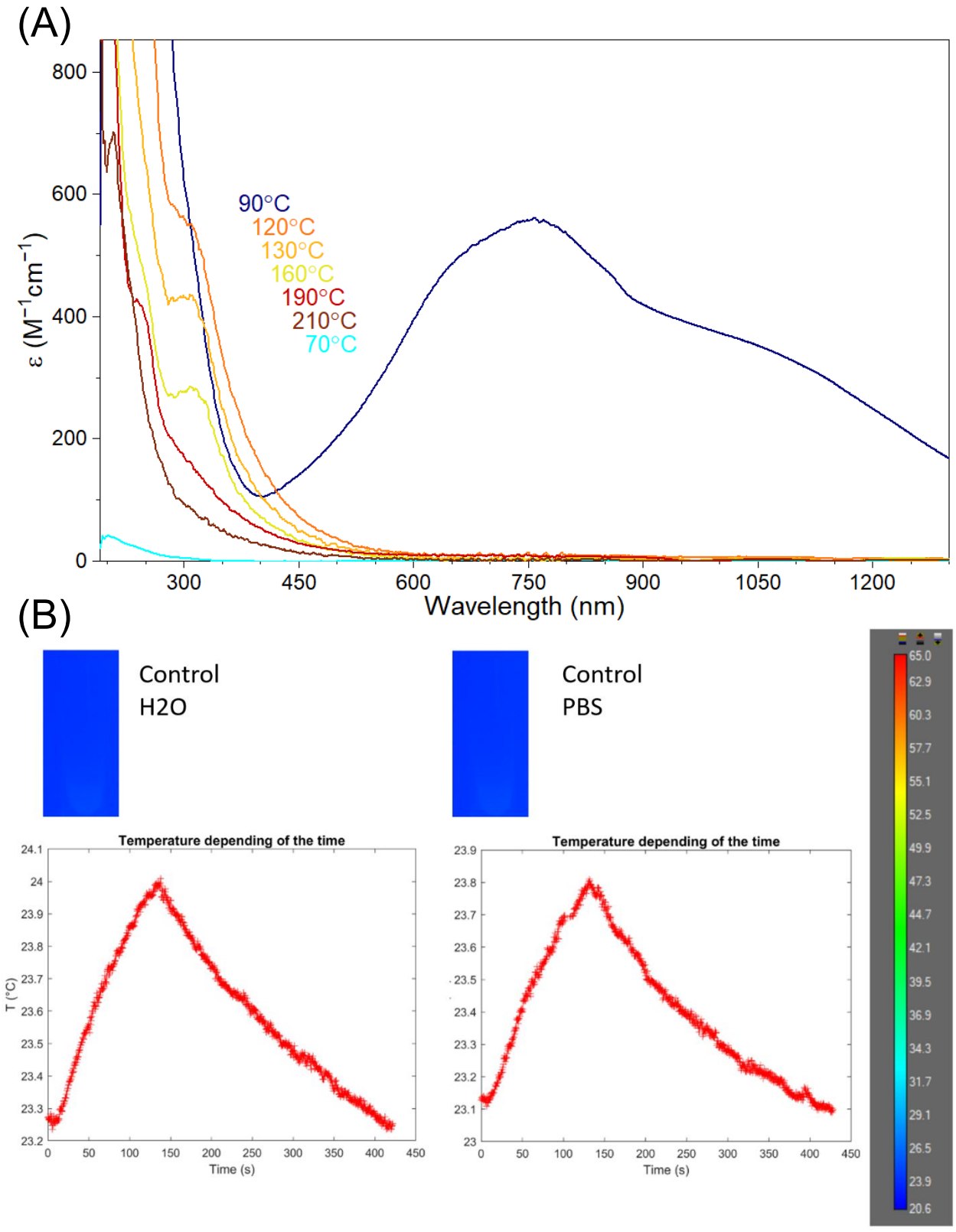

Figure S8 Molar attenuation coefficient of MoO_X nanoclusters prepared at different temperatures (A). Thermal map and heating curves for control H_2O and PBS samples for the PTT experiment (B). Negligible heating of around 0.7 °C was achieved after 2 minutes of irradiation by 0.5 W power.

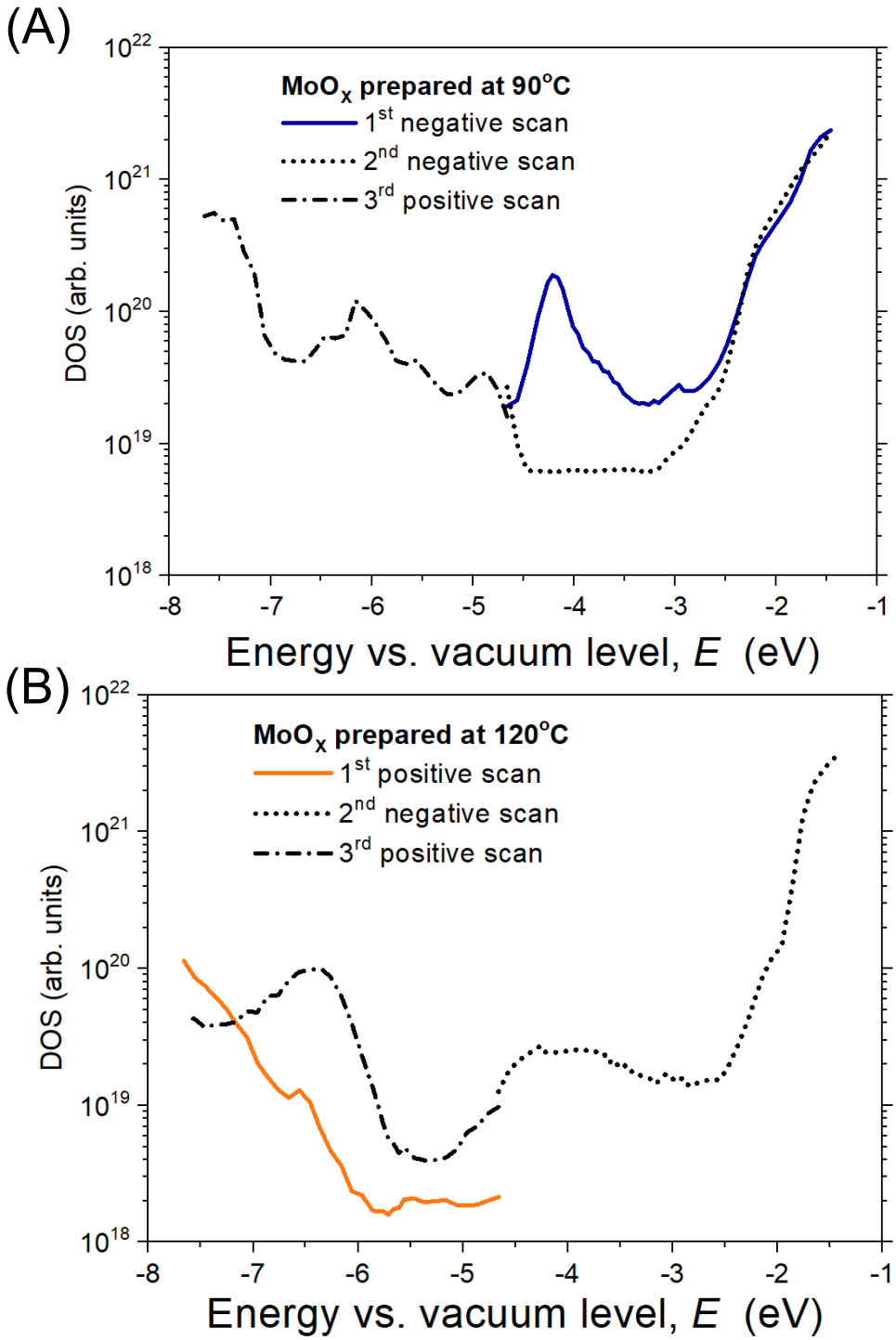

Figure S9 DOS changes induced by ER-EIS scans in layers of MoO_X nanoparticles prepared at 90 °C (A) and 120 °C (B). A positive scan at MoO_X prepared at 90 °C induces DOS changes that lead to a spectrum similar to that of MoO_X prepared at 120 °C. On the other hand, the negative scan of MoO_X prepared at 120 °C leads to DOS distribution similar to MoO_X prepared at 90 °C. Corresponding changes in absorption are shown in Figure S10.

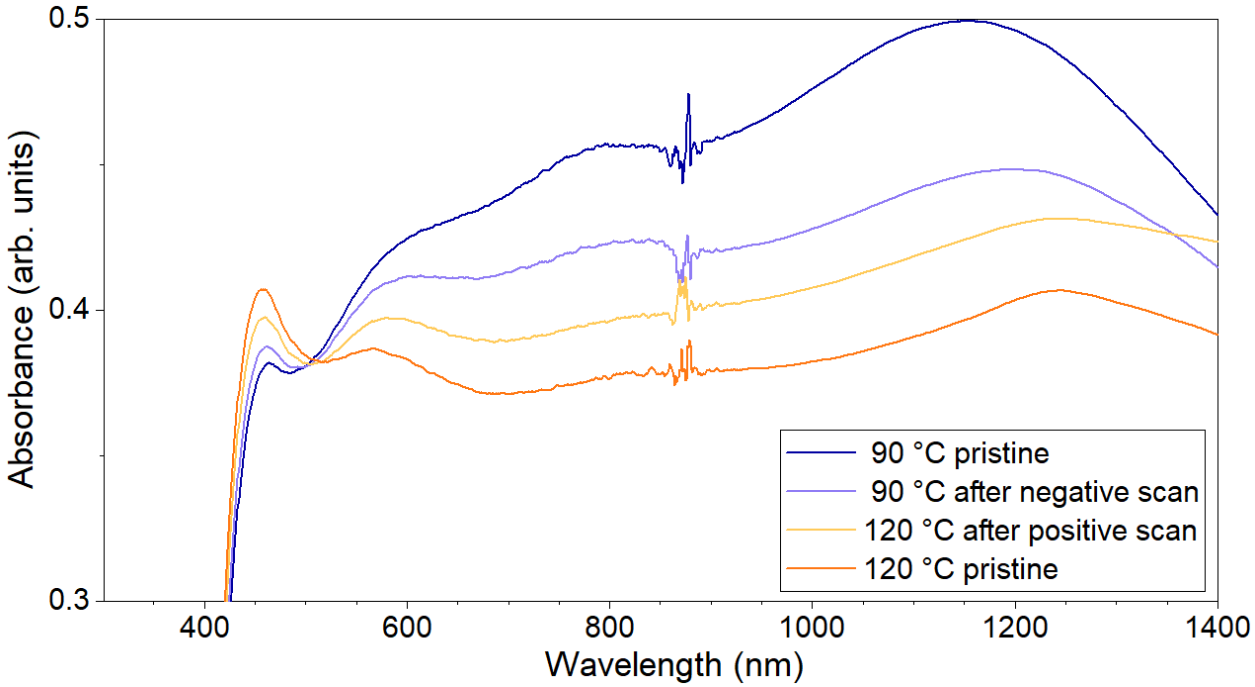

Figure S10 Absorbance spectrum of 90 °C and 120 °C sample layers on ITO before and after ER-EIS scans. Decrease in absorbance can be seen in 90 °C sample after the positive scan, whereas for 120 °C sample, the absorption in sub-bandgap energies is increased compared to pristine sample due to increase in intermediate defect states in Figure S5. Disruption around 875 nm is an artifact caused by an optical instrumentation change of the spectrometer.

Table S1. Apparent surface chemical composition of three points of MoO_X 70°C.

MoOx 70°C	Surface chemical composition (at.%)				
	Mo3d $Mo^{4+}/Mo^{5+}/Mo^{6+}$	O1s I/II/III	C1s sp2/sp3/I/II/III/IV	*N1s*	Si2p/K2p
1	6.0 0.1/1.7/4.2	55.2 6.8/8.6/39.8	21.5 5.9/8.8/4.5/0.9/0.8/0.6	*0.5*	16.8/-
2	4.4 -/1.3/3.1	56.6 5.6/6.0/45.0	21.4 4.4/9.3/4.8/1.0/0.7/1.2	*0.5*	16.9/0.3
3	9.2 0.1/2.9/6.2	52.9 7.3/15.5/30.1	26.1 8.4/7.7/5.9/1.8/1.0/1.3	*0.6*	10.9/0.3

C1s: I = C-O ~ 286 eV, II = C=O ~ 287 eV, III = O-C-O/NC=O ~ 288 eV, IV: OC=O ~ 289 eV
O1s: I= O^{2-}/C=O ~ 531 eV, II= C-O ~ 532 eV, III= O-C-O/Si-O ~ 533 eV

Table S2. Apparent surface chemical composition of three points of MoO_X 90°C.

MoOx 90°C	Surface chemical composition (at.%)				
	Mo3d $Mo^{4+}/Mo^{5+}/Mo^{6+}$	O1s I/II/III	C1s sp2/sp3/I/II/III/IV	*N1s*	Si2p/K2p
1	14.4 0.1/4.8/9.5	44.6 0.9/30.6/13.1	39.1 10.4/17.2/7.0/2.4/1.3/0.8	*1.0*	-/0.9
2	14.5 0.1/5.3/9.1	45.4 1.0/31.0/13.4	38.4 8.8/17.7/7.0/2.5/1.7/0.7	*1.0*	-/0.8
3	14.7 0.1/5.5/9.1	45.9 1.1/31.2/13.6	37.6 9.0/16.9/6.9/2.5/1.6/0.7	*1.1*	-/0.7

C1s: I = C-O ~ 286 eV, II = C=O ~ 287 eV, III = O-C-O/NC=O ~ 288 eV, IV: OC=O ~ 289 eV
O1s: I= O^{2-}/C=O ~ 531 eV, II= C-O ~ 532 eV, III= O-C-O/Si-O ~ 533 eV

Table S3. Apparent surface chemical composition of three points of MoO_X 120°C.

MoOx 120°C	Surface chemical composition (at.%)				
	Mo3d $Mo^{4+}/Mo^{5+}/Mo^{6+}$	O1s I/II/III	C1s sp2/sp3/I/II/III/IV	*N1s*	Si2p/K2p
1	13.3 0.2/11.1/2.0	44.5 0.7/37.0/6.8	41.0 11.9/14.3/7.2/4.7/1.0/1.9	*1.2*	-/-
2	13.7 0.2/11.6/1.9	45.6 0.6/38.3/7.0	39.0 10.6/13.9/8.2/3.7/0.8/1.8	*1.4*	-/-
3	13.8 0.2/11.6/2.0	45.8 0.5/38.4/6.9	39.2 9.5/15.1/7.2/3.9/2.1/1.4	*1.2*	-/-

C1s: I = C-O ~ 286 eV, II = C=O ~ 287 eV, III = O-C-O/NC=O ~ 288 eV, IV: OC=O ~ 289 eV
O1s: I= O^{2-}/C=O ~ 531 eV, II= C-O ~ 532 eV, III= O-C-O/Si-O ~ 533 eV

Table S4. Apparent surface chemical composition of three points of MoO_X 140°C.

MoOx 140°C	Surface chemical composition (at.%)				
	Mo3d $Mo^{4+}/Mo^{5+}/Mo^{6+}$	O1s I/II/III	C1s sp2/sp3/I/II/III/IV	*N1s*	Si2p/K2p
1	14.2 0.2/10.7/3.3	45.0 0.4/38.1/6.5	39.0 8.7/18.6/5.4/3.9/1.1/1.3	*1.3*	0.5/-
2	14.4 0.2/11.1/3.1	45.4 0.5/38.5/6.4	38.6 10.0/16.4/6.1/3.0/1.9/1.2	*1.1*	0.5/-
3	14.4 0.2/11.0/3.2	45.6 0.4/38.6/6.6	38.3 10.0/15.9/6.7/2.9/1.3/1.5	*1.2*	0.5/-

C1s: I = C-O ~ 286 eV, II = C=O ~ 287 eV, III = O-C-O/NC=O ~ 288 eV, IV: OC=O ~ 289 eV
O1s: I= O^{2-}/C=O ~ 531 eV, II= C-O ~ 532 eV, III= O-C-O/Si-O ~ 533 eV

Table S5. Apparent surface chemical composition of three points of MoO_X 150°C.

MoOx 150°C	Surface chemical composition (at.%)				
	Mo3d $Mo^{4+}/Mo^{5+}/Mo^{6+}$	O1s I/II/III	C1s sp2/sp3/I/II/III/IV	*N1s*	Si2p/K2p
1	12.3 0.2/10.9/1.2	41.8 0.5/34.6/6.7	44.0 7.1/23.6/6.0/4.6/0.6/2.1	*1.7*	-/0.2
2	12.9 0.2/11.6/1.1	43.6 0.6/36.4/6.6	41.7 6.1/21.9/7.3/3.7/0.8/1.9	*1.6*	-/0.2
3	12.7 0.2/11.3/1.2	42.7 0.4/35.7/6.6	42.8 6.9/21.5/7.5/3.9/1.0/2.0	*1.6*	-/0.2

C1s: I = C-O ~ 286 eV, II = C=O ~ 287 eV, III = O-C-O/NC=O ~ 288 eV, IV: OC=O ~ 289 eV
O1s: I= O^{2-}/C=O ~ 531 eV, II= C-O ~ 532 eV, III= O-C-O/Si-O ~ 533 eV

Table S6. Apparent surface chemical composition of three points of MoO_X 160°C.

MoOx 160°C	Surface chemical composition (at.%)				
	Mo3d $Mo^{4+}/Mo^{5+}/Mo^{6+}$	O1s I/II/III	C1s sp2/sp3/I/II/III/IV	*N1s*	Si2p/K2p
1	12.7 0.2/10.9/1.6	42.9 0.5/35.3/7.1	43.3 9.1/18.0/8.9/3.6/1.3/2.4	*1.3*	-/-
2	13.0 0.2/11.4/1.4	43.6 0.3/36.3/7.0	42.2 9.5/17.8/7.7/4.0/0.9/2.3	*1.2*	-/-
3	12.9 0.2/11.3/1.4	42.9 0.4/35.9/6.6	43.1 10.4/18.6/6.1/4.6/1.0/2.4	*1.2*	-/-

C1s: I = C-O ~ 286 eV, II = C=O ~ 287 eV, III = O-C-O/NC=O ~ 288 eV, IV: OC=O ~ 289 eV
O1s: I= O^{2-}/C=O ~ 531 eV, II= C-O ~ 532 eV, III= O-C-O/Si-O ~ 533 eV

Table S7. Apparent surface chemical composition of three points of MoO_X 190°C.

MoOx 190°C	Surface chemical composition (at.%)				
	Mo3d $Mo^{4+}/Mo^{5+}/Mo^{6+}$	O1s I/II/III	C1s sp2/sp3/I/II/III/IV	*N1s*	Si2p/K2p
1	10.5 -/8.5/2.0	36.9 1.2/26.4/9.3	51.8 11.9/26.9/7.2/3.8/0.5/1.5	*0.2*	0.6/-
2	10.7 -/9.1/1.6	38.0 1.6/26.5/9.9	50.5 15.2/22.7/7.9/2.8/0.5/1.4	*0.2*	0.8/-

C1s: I = C-O ~ 286 eV, II = C=O ~ 287 eV, III = O-C-O/NC=O ~ 288 eV, IV: OC=O ~ 289 eV
O1s: I= O^{2-}/C=O ~ 531 eV, II= C-O ~ 532 eV, III= O-C-O/Si-O ~ 533 eV

Table S8. Apparent surface chemical composition of three points of MoO_X 210°C.

MoOx 210°C	Surface chemical composition (at.%)				
	Mo3d $Mo^{4+}/Mo^{5+}/Mo^{6+}$	O1s I/II/III	C1s sp2/sp3/I/II/III/IV	*N1s*	Si2p/K2p
1	11.7 -/10.0/1.7	39.1 2.7/30.1/6.3	47.3 15.3/21.3/5.8/2.8/0.7/1.4	*2.0*	-/-
2	6.7 -/6.0/0.7	36.9 2.6/15.6/18.7	54.8 12.0/19.8/10.6/6.9/3.2/2.3	*1.2*	0.4/-
3	10.4 -/9.3/1.1	37.1 2.9/27.0/7.2	50.4 11.8/26.0/8.4/1.5/0.7/2.0	*1.7*	0.4/-

C1s: I = C-O ~ 286 eV, II = C=O ~ 287 eV, III = O-C-O/NC=O ~ 288 eV, IV: OC=O ~ 289 eV
O1s: I= O^{2-}/C=O ~ 531 eV, II= C-O ~ 532 eV, III= O-C-O/Si-O ~ 533 eV

Table S9. Apparent surface chemical composition of three points of reference microcrystalline MoO_2.

MoO_2	Surface chemical composition (at.%)				
	Mo3d $Mo^{4+}/Mo^{5+}/Mo^{6+}$	O1s I/II/III	C1s sp2/sp3/I/II/III/IV	*N1s*	Si2p/K2p
1	20.0 5.6/11.0/3.4	47.8 29.3/14.0/4.5	30.0 10.5/10.4/5.3/1.1/1.6/1.5	*1.4*	-/0.5
2	20.8 5.6/11.2/3.3	48.4 26.6/18.3/3.5	28.9 9.1/9.4/5.9/1.2/1.2/2.1	*1.7*	-/0.7
3	19.1 5.0/10.6/3.5	46.7 26.0/17.4/3.3	30.0 10.3/11.7/6.0/1.2/1.7/1.5	*1.3*	-/0.7

C1s: I = C-O ~ 286 eV, II = C=O ~ 287 eV, III = O-C-O/NC=O ~ 288 eV, IV: OC=O ~ 289 eV
O1s: I= O^{2-}/C=O ~ 531 eV, II= C-O ~ 532 eV, III= O-C-O/Si-O ~ 533 eV